Wave-equation Reflection Traveltime Inversion

Sanzong Zhang, Gerard Schuster, King Abdullah University of Science and Technology,
and Yi Luo, Saudi Aramco*

SUMMARY

The main difficulty with iterative waveform inversion using a gradient optimization method is that it tends to get stuck in local minima associated within the waveform misfit function. This is because the waveform misfit function is highly non-linear with respect to changes in the velocity model. To reduce this nonlinearity, we present a reflection traveltime tomography method based on the wave equation which enjoys a more quasi-linear relationship between the model and the data. A local crosscorrelation of the windowed downgoing direct wave and the upgoing reflection wave at the image point yields the lag time that maximizes the correlation. This lag time represents the reflection traveltime residual that is back-projected into the earth model to update the velocity in the same way as wave-equation transmission traveltime inversion. No travel-time picking is needed and no high-frequency approximation is assumed. The mathematical derivation and the numerical examples are presented to partly demonstrate its efficiency and robustness.

INTRODUCTION

Prestack depth migration of 3D seismic data is the industry standard for computing detailed estimates of the earth's reflectivity distribution. However, an accurate velocity model is a precondition for imaging complex geological structures. To estimate this velocity model, there are three primary inversion methods: migration velocity analysis (MVA), traveltime inversion, and full waveform inversion. For migration velocity analysis (Symes and Kern, 1994; Sava and Biondi, 2004; Shen and Calandra, 2005), the optimal migration velocity is the one that best flattens the reflection events in a common image gather. For traveltime inversion (Dines and Lytle, 1979; Paulsson et al., 1985; Ivansson, 1985; Bishop et al., 1985; Lines, 1988), the traveltimes of refraction and reflection arrivals are used to invert for smooth features of the velocity model, while full waveform inversion (Tarantola, 1986, 1987; Mora, 1987; Crase et al., 1992; Zhou et al., 1995; Pratt, 1998) inverts the waveform information for fine details of the earth model.

A more detailed analysis shows that traveltime inversion is constrained by a high-frequency approximation, and so it fails to invert for the earth's velocity variations having nearly the same wavelength or less than that of the source wavelet. Consequently, the resolution of the velocity model constructed from the traveltimes is much less than that of full waveform inversion. The merit is that the traveltime misfit function (normed squared error between observed and calculated traveltimes) is quasi-linear with respect to velocity perturbations so that an efficient velocity inversion can be achieved even if the starting model is far from the actual model (Luo and Schuster,

1991a and 1991b; Zhou et al., 1995). Although very sensitive to the choice of starting models or noisy amplitudes, full waveform inversion can sometimes reconstruct a finely detailed estimation of the earth model. This is because there is no high-frequency assumption about the data, and almost all seismic events are embedded in the misfit function. The problem with full waveform inversion, however, is that its misfit function (normed squared error between the observed and synthetic seismograms) can be highly nonlinear with respect to changes in the velocity model. In this case, a gradient method will tend to get stuck in a local minima if the starting model is far away from the actual model.

To exploit the strengths and ameliorate the weaknesses of both ray-based traveltime tomography and full waveform inversion, wave-equation-based traveltime inversion was developed to invert the velocity model (Luo and Schuster, 1991a and 1991b; Zhou et al, 1995; Zhang and Wang, 2009; Leeuwen and Mulder, 2010). This kind of inversion methods inverts traveltime using the gradient calculated from the wave equation. It is not constrained by a high-frequency approximation and traveltime picking is not necessary. Other important benefits are a convergence rate that is somewhat insensitive to the starting model, a high degree of model resolution, and a robustness in the presence of data noise. However, these traveltime inversion methods are designed to invert transmission waves in seismic data, and are not designed to invert the reflection traveltimes. Unlike refraction and direct waves, reflection waves can provide more velocity information about the deeper subsurface for model inversion. However, full waveform inversion of reflection wave is difficult if the initial velocity model is far from the true model. To overcome this limitation, this paper presents the extension of wave-equation transmission traveltime inversion (WTI) (Luo and Schuster, 1991a and 1991b) to wave-equation reflection traveltime inversion (WRTI).

This paper is organized into three sections. The first section describes the basic theory of image-domain wave-equation reflection traveltime inversion. The second section shows numerical examples to verify the effectiveness of this method. The last section draws some conclusions.

THEORY

The key step in WRTI is to transform the reflection data into that recorded by a virtual transmission experiment. This transmission data can then be inverted by WTI (Luo and Schuster,1991a).

1). Assume an initial velocity model.

2). Migrate the recorded upgoing reflection data to get the image points at $\mathbf{x}$.

3). Forward propagate the source at $\mathbf{x}_s$ to $\mathbf{x}$ to get the downgoing direct wave $p_s(\mathbf{x},t)$ as shown in Figure 1(a). Now we have the virtual source wavelet $p_s(\mathbf{x},t)$ where the virtual source is

at **x**, which will be used to update the velocity on the receiver side.

4). Backpropagate the observed reflection data from $\mathbf{x}_g$ to the image point **x** and get the upgoing reflection wave $p_g(\mathbf{x},t)$ as shown in Figure 1(b). Now we have the virtual reflection data at **x** which can be used to find the the traveltime difference between the downgoing direct wave $p_s(\mathbf{x},t)$ and the upgoing reflection wave $p_g(\mathbf{x},t)$.

5). Crosscorrelate the downgoing direct event in $p_s(\mathbf{x},t)$ and the upgoing reflection event in $p_g(\mathbf{x},t)$ to find the time shift $\Delta\tau$ between them as shown in Figure 1(c).

6). Update the velocity model by smearing $\Delta\tau$ along the weighted wavepath between $\mathbf{x}_s$ and **x** and between **x** and $\mathbf{x}_g$ as shown in Figure 1(d). This step is actually the application of WTI to the virtual transmission data.

7). Repeat steps (3)-(6) for all source and image points.

8). Go back to step (2) until the norm of the traveltime residual satisfies the specified minimum.

In summary, WRTI can be decomposed into two steps. The first step is to redatum the geophones from the free surface to the image points. The second step is to redatum the source to the image point. Hence, two virtual transmission experiments are formed and used to update the velocity model. The potential benefit is that reflection traveltime inversion might enjoy robust convergence properties and not require the tedious picking of reflection traveltimes.

(a) Forward extrapolate source

(b) Backward extrapolate geophones

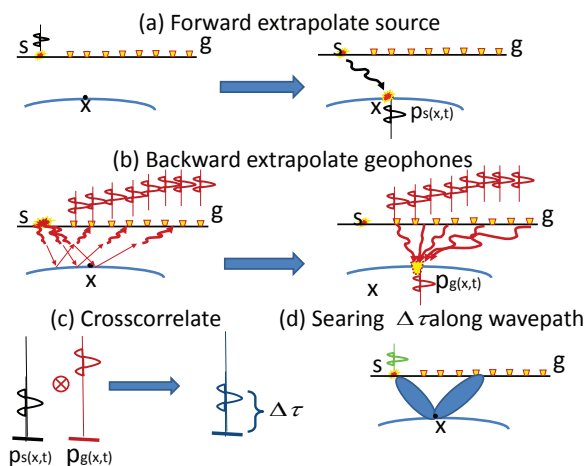(c) Crosscorrelate (d) Searing $\Delta\tau$ along wavepath

Figure 1: (a). The forward extrapolation of the source field. (b). The backward extrapolation of the geophone field. (c). The crosscorrelation of the downgoing direct wave and the upgoing reflection wave. (d). The misfit gradient is propertial to the $\Delta\tau$ weighted wavepath functions between the source and the image points, and the image point and the geophones.

Connective function

The following analysis assumes that the propagation of seismic waves honors the 2-D acoustic wave equation. Let $p(\mathbf{x}_r,t|\mathbf{x}_s)_{obs}$ be the pressure at time t observed at the receiver location $\mathbf{x}_r$ due to a source at $\mathbf{x}_s$. The source is always assumed to be initiated at zero time. For a given velocity model, $p(\mathbf{x}_r,t|\mathbf{x}_s)_{cal}$ denotes the calculated seismogram that honors the 2D acoustic wave equation. The crosscorrelation function between the

forward wavefield and the backward wavefield can be used to determine the image at **x**

$$f(\mathbf{x},\tau) = \int dt\, p_s(\mathbf{x},t+\tau)p_g(\mathbf{x},t), \qquad (1)$$

where $p_s(\mathbf{x},t+\tau)$ is the forward wavefield initiated by the source at $\mathbf{x}_s$

$$p_s(\mathbf{x},t) = p(\mathbf{x},t|\mathbf{x}_s)_{cal} = w(t) * g(\mathbf{x},t|\mathbf{x}_s,0). \qquad (2)$$

Here $w(t)$ is the source wavelet, and $g(\mathbf{x},t|\mathbf{x}_s,0)$ is the Green's function. $p_g(\mathbf{x},t)$ is the backward wavefield by the time-reversed propagation of the observed data $p(\mathbf{x}_g,t|\mathbf{x}_s)_{obs}$

$$p_g(\mathbf{x},t) = \int p(\mathbf{x}_g,t|\mathbf{x}_s)_{obs} * g(\mathbf{x},-t|\mathbf{x}_g,0)d\mathbf{x}_g, \qquad (3)$$

and τ is the time lag of the crosscorrelation function. When $\tau = 0$, equation (2) is the conventional correlation imaging condition. The nonzero time lag indicates the inaccuracy of the velocity model. The extremum of $f(\mathbf{x},\tau)$ should satisfy

$$f(\mathbf{x},\Delta\tau) = max\{f(\mathbf{x},\tau)|\tau \in [-T,T]\} \qquad (4)$$

or

$$f(\mathbf{x},\Delta\tau) = min\{f(\mathbf{x},\tau)|\tau \in [-T,T]\}, \qquad (5)$$

where T is the estimated maximum time lag between the forward modeled wave from the source and the backward propagated wave from the receivers. Note $\Delta\tau = 0$ indicates that the correct velocity model has been found which generates a downgoing direct wave and upgoing reflection wave arriving at the same time. The derivative of $f(\mathbf{x},\tau)$ with respect to τ should be zero at $\Delta\tau$ unless its maximum or minimum is at an end point T or $-T$:

$$\dot{f}_{\Delta\tau} = \frac{\partial f(\mathbf{x},\tau)}{\partial\tau}|_{\tau=\Delta\tau} = \int dt\, \dot{p}_s(\mathbf{x},t+\tau)p_g(\mathbf{x},t) = 0, \quad (6)$$

where $\dot{p}_s(\mathbf{x},t+\tau)$ represents the time derivative of the calculated downgoing wave.

Misfit function

The inverse problem is defined as finding a velocity model that minimizes the following misfit function:

$$S = \frac{1}{2}\sum_s\sum_x (\Delta\tau)^2. \qquad (7)$$

Here **x** is the image point, and **s** is the source position. The reflection traveltime inversion is computed by finding $c(\mathbf{x}')$ that minimizing the sum of the squared traveltime residuals. For simplicity, a steepest descent non-linear optimization method is used to describe the iterative minimization of equation (7), with the understanding that a preconditioned conjugate gradient method is used in practice. To update the velocity model, the steepest descent method gives

$$c_{k+1}(\mathbf{x}') = c_k(\mathbf{x}') + \alpha_k \cdot \gamma_k(\mathbf{x}'), \qquad (8)$$

Wave-equation Reflection Traveltime Inversion

where $\gamma_k(\mathbf{x}')$ is the steepest descent direction for the misfit function S, $\mathbf{x}'$ represents any location in the velocity model, α_k is the step length, and k denotes the kth iteration.

Gradient function

Taking the Frechĕt derivative of S with respect to velocity perturbations yields the misfit gradient

$$\gamma(\mathbf{x}') = -\frac{\partial S}{\partial c(\mathbf{x}')} = -\sum_\mathbf{s} \sum_\mathbf{x} \Delta\tau \frac{\partial(\Delta\tau)}{\partial c(\mathbf{x}')}, \qquad (9)$$

where $\gamma(\mathbf{x}')$ represents the traveltime misfit gradient. Using (6) and the rule for an implicit function derivative, we get

$$\frac{\partial(\Delta\tau)}{\partial c(\mathbf{x}')} = -\frac{\frac{\partial(\dot{f}_{\Delta\tau})}{\partial(c(\mathbf{x}'))}}{\frac{\partial(\dot{f}_{\Delta\tau})}{\partial(\Delta\tau)}}, \qquad (10)$$

where

$$E = \frac{\partial(\dot{f}_{\Delta\tau})}{\partial(\Delta\tau)} = \int \ddot{p}_s(\mathbf{x}, t+\Delta\tau) p_g(\mathbf{x}, t) dt, \qquad (11)$$

and

$$\frac{\partial(\dot{f}_{\Delta\tau})}{\partial(c(\mathbf{x}'))} = \int \left[\frac{\partial p_g(\mathbf{x}, t)}{\partial c(\mathbf{x}')} \dot{p}_s(\mathbf{x}, t+\Delta\tau) + \frac{\partial \dot{p}_s(\mathbf{x}, t+\Delta\tau)}{\partial c(\mathbf{x}')} p_g(\mathbf{x}, t) \right] dt, \qquad (12)$$

where E is the constant. Under the Born approximation, we can rewrite the misfit gradient (10) as

$$\gamma(\mathbf{x}') = \frac{1}{c(\mathbf{x}')^3} \sum_\mathbf{s} \sum_\mathbf{x} \int \overbrace{\left[\frac{\Delta\tau}{E} p_g(\mathbf{x}, t) * \ddot{g}(\mathbf{x}', -t-\Delta\tau | \mathbf{x}, 0) \right]}^{\text{Backpropagation of the redatumed data}}$$

$$\overbrace{\left[\dot{p}(\mathbf{x}', t+\Delta\tau | \mathbf{x}_s)_{cal} \right]}^{\text{Forward propagation of the source}} dt +$$

$$\frac{1}{c(\mathbf{x}')^3} \sum_\mathbf{s} \sum_\mathbf{x} \int \overbrace{\left[\int \frac{\Delta\tau}{E} p(\mathbf{x}_g, t | \mathbf{x}_s)_{obs} * \dot{g}(\mathbf{x}', -t | \mathbf{x}_g, 0) d\mathbf{x}_g \right]}^{\text{Backpropagation of the observed data}}$$

$$\overbrace{\left[\dot{p}(\mathbf{x}, t+\Delta\tau | \mathbf{x}_s)_{cal} * \dot{g}(\mathbf{x}', t | \mathbf{x}, 0) \right]}^{\text{Forward propagation of the redatumed source}} dt. \qquad (13)$$

Equation (13) indicates that the gradient function of WRTI inversion consists of two gradient functions of WTI for two virtual transmission experiments. One virtual seismic experiment is where the geophones are redatumed to the image point, and the source is on the free surface. The other one is where the source are redatumed to the image point, and the geophones are still on the free surface. The velocity model is updated by smearing the time shifts at the image point along the wavepath between the source and the image point, and the image point and the geophones.

NUMERICAL EXAMPLES

The first example is associated with a three-layer model. The model in Figure 2(a) is discretized into a mesh with 201x401 gridpoints, with 100 line sources and 401 receivers on the top surface of the model, respectively. A 40-gridpoint wide absorbing sponge zone is added along each side, and the grid interval is 20 meters. The source wavelet is a Ricker wavelet with a peak frequency of 10 Hz, and the starting model is shown in Figure 2(b) which is a constant velocity model. The observed seismograms are generated by a fourth-order finite-difference solution to the 2D acoustic wave equation (with constant density). Figure 2(c) is a typical shot gather recorded on the free surface, where the direct wave is removed. The observed data is redatumed from the free surface to the reflectors as shown in Figure 2(d). Figure 2(e) shows the forward modeled wavefield recorded on two reflectors. A time window is used to separate out the downgoing direct wave and the upgoing reflection wave from the calculated data and the redatumed data indicated by the dashed lines in Figure 2(d) and Figure 2(e). The first arrival traveltime at reflectors calculated from the eikonal solver is consistent with the center of the time window. The direct downgoing waves are cross-correlated with the corresponding redatumed reflection waves to find the time shift between them. The inversion result after seven iterations are shown in Figure 2(f). It shows that wave-equation reflection traveltime inversion is an efficient way to construct the velocity model. Next, we test our inversion algorithm on a more practical fault model. Figure 3(a) displays the fault model which has several nearly horizontal layers and a steep fault. The starting model shown in Figure 3(b) is obtained by smoothing the true model. The inversion result after five iterations is illustrated in Figure 3(c). It is clear that details present in the original model such as the fault and the thin layer become visible in the inverted model.

CONCLUSION

A new seismic reflection traveltime tomography is presented which reconstructs velocities from reflection traveltimes computed from solutions to the wave equation. No high-frequency assumption to the data is needed, and traveltime picking and event identification are sometimes unnecessary. The mathematical derivation demonstrates that WRTI is roughly equivalent to that of transmission tomography for two virtual transmission experiments. The synthetic data tests illustrate that it converges robustly in the simple model inverion. The limitation of this method is that some approximate reflection points must be known before inversion. In practice, it can be overcomed by combining this method with MVA.

ACKNOWLEDGMENTS

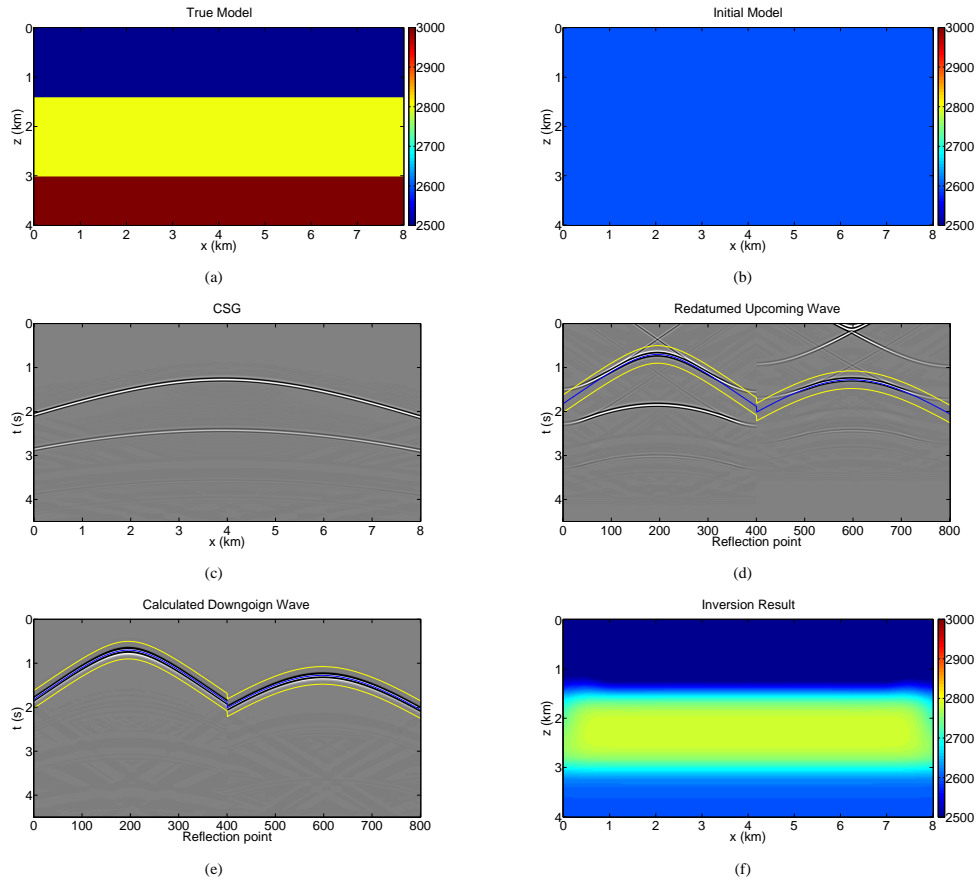# Wave-equation Reflection Traveltime Inversion

Figure 2: (a). Three-layer true velocity model. (b). The initial constant velocity model. (c). The observed data. The direct wave is removed. (d). The upgoing reflection wave which is obtained by redatuming the observed data from the free surface to the reflectors. (e). The calculated downgoing wave on the reflectors. (f). The inversion result after seven iterations.
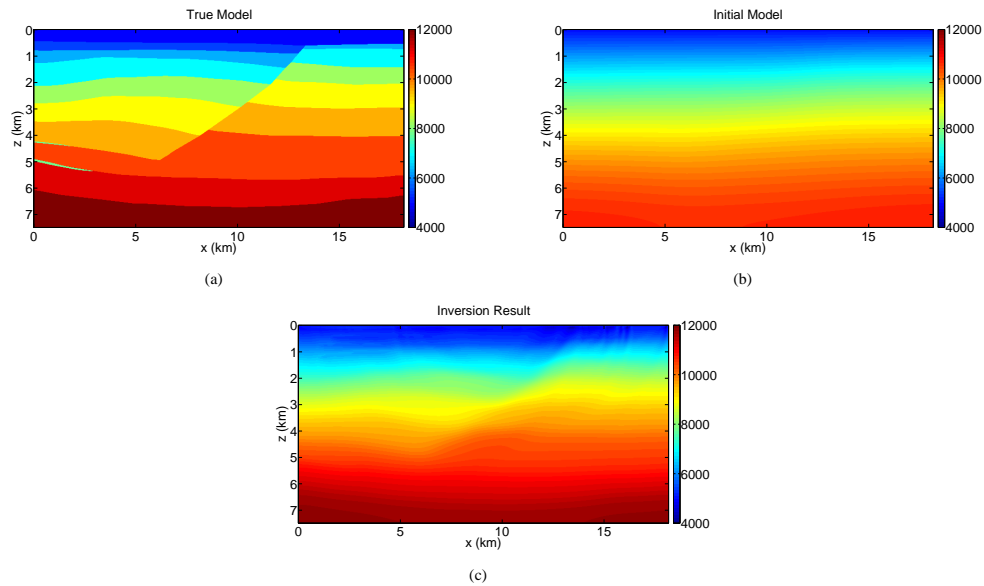

Figure 3: (a). The true velocity model with a fault. (b). The initial velocity model. (c). The inversion result after ten iterations.

EDITED REFERENCES

Note: This reference list is a copy-edited version of the reference list submitted by the author. Reference lists for the 2011 SEG Technical Program Expanded Abstracts have been copy edited so that references provided with the online metadata for each paper will achieve a high degree of linking to cited sources that appear on the Web.

REFERENCES

Bishop, T., K. Bube, R. Cutler, R. Langan, P. Love, J. Resnick, R. Shuey, D. Spindler, and H. Wyld, 1985, Tomographic determination of velocity and depth in laterally varying media: Geophysics, **50**, 903–923, doi:10.1190/1.1441970.

Crase, E., C. Wideman, M. Noble, and A. Tarantola, 1992, Nonlinear elastic waveform inversion of land seismic reflection data: Journal of Geophysics Research, **97**, 4685–4704.

Dines, K., and R. Lytle, 1979, Computerized geophysical tomography: Proceedings of the IEEE, **67**, 1065–1073, doi:10.1109/PROC.1979.11390.

Ivansson, S., 1985, A study of methods for tomographic velocity estimation in the presence of low-velocity zones: Geophysics, **50**, 969–988, doi:10.1190/1.1441975.

Levander, A. R., 1988, Fourth-order finite-difference P-SV seismograms: Geophysics, **53**, 1425–1436, doi:10.1190/1.1442422.

Lines, L., 1988, Inversion of geophysical data: SEG Geophysics Reprint Series No. 9.

Luo, Y., and G. Schuster, 1991a, Wave equation traveltime inversion: Geophysics, **56**, 645–653, doi:10.1190/1.1443081.

Luo, Y., and G. Schuster, 1991b, Wave equation inversion of skeletonized geophysical data: Geophysical Journal International, **105**, 289–294, doi:10.1111/j.1365-246X.1991.tb06713.x.

Mora, P., 1987, Nonlinear two-dimensional elastic inversion of multioffset seismic data: Geophysics, **52**, 1211–1228, doi:10.1190/1.1442384.

Paulsson, B., N. Cook, and T. McEvilly, 1985, Elastic wave velocities and attenuation in an underground granitic repository for nuclear waste: Geophysics, **50**, 551–570, doi:10.1190/1.1441932.

Pratt, R. G., C. Shin, and G. J. Hicks, 1998, Gauss-Newton and full Newton methods in frequency-space seismic waveform inversion: Geophysical Journal International, **133**, 341–362, doi:10.1046/j.1365-246X.1998.00498.x.

Sava, P., and B. Biondi, 2004, Wave-equation migration velocity analysis, I: Theory: Geophysical Prospecting, **52**, 593–606.

Shen, P., and H. Calandra, 2005, One-way waveform inversion within the framework of adjoint state differential migration: 75th Annual International Meeting, SEG, Expanded Abstracts, 1709–1712.

Symes, W., and M. Kern, 1994, Inversion of reflection seismograms by differential semblance analysis: Algorithm structure and synthetic examples: Geophysical Prospecting, **42**, 565–614, doi:10.1111/j.1365-2478.1994.tb00231.x.

Tarantola, A., 1986, A strategy for nonlinear elastic inversion of seismic reflection data: Geophysics, **51**, 1893–1903, doi:10.1190/1.1442046.

Tarantola, A., 1987, Inverse problem theory: Elsevier.

van Leeuwen, T., and W. A. Mulder, 2010, A correlation-based misfit criterion for wave-equation traveltime tomography: Geophysical Journal International, **182**, 1383–1394, doi:10.1111/j.1365-246X.2010.04681.x.

Zhou, C., W. Cai, Y. Luo, G. Schuster, and S. Hassanzadeh, 1995, Acoustic wave-equation traveltime and waveform inversion of crosshole seismic data: Geophysics, **60**, 765–773, doi:10.1190/1.1443815.